

# MEASUREMENTS OF COPPER RF SURFACE RESISTANCE AT CRYOGENIC TEMPERATURES FOR APPLICATIONS TO X-BAND AND S-BAND ACCELERATORS\*

A. Cahill<sup>†</sup>, A. Fukasawa, J. Rosenzweig, UCLA, Los Angeles, California

Y. Higashi OIST, Onna-son, Okinawa, Japan

G. B. Bowden, V.A. Dolgashev, J. Guo<sup>1</sup>, M. Franzi, S. Tantawi,

P. B. Welander, C. Yoneda, SLAC, Menlo Park, CA, USA

<sup>1</sup>Now at JLab, Newport News, Virginia, USA

## Abstract

Recent SLAC experiments with cryogenically cooled X-band standing wave copper accelerating cavities have shown that these structures can operate with accelerating gradients of 250 MV/m and low breakdown rates. These results prompted us to perform systematic studies of copper rf properties at cryogenic temperatures at low rf power. We placed copper cavities into a cryostat with a cryocooler, so the cavities could be reduced to 4K. We used different shapes of cavities for the X-band and S-band measurements. RF properties of the cavities were measured using a network analyzer. We calculated rf surface resistance from measured  $Q_0$  at temperatures from 4 K to room temperature. The results were then compared to the theory proposed by Reuter and Sondheimer. These measurements are part of studies with the goal of reaching very high operating accelerating gradients in normal conducting rf structures.

## MOTIVATION

There is a large push in accelerator technology to reach higher gradients. To increase the gradient, efforts were made to understand the physics of rf breakdown. The rf breakdowns are a major limiting factor in reaching higher gradients in normal conducting copper. During the NLC/GLC work the statistical nature of rf breakdown became apparent [1–4]. For most accelerating structures exposed to the same rf power and pulse shape, the number of rf breakdowns per pulse is nearly steady or slowly decreasing over  $10^5 - 10^7$  pulses. The breakdown probability became one of the main quantitative requirements characterizing high gradient performance of linacs.

Presently, X-band structures are the most studied in terms of rf breakdowns [4–8]. We know that breakdown statistics depend on pulse heating [9] and a numerous list of other factors, such as the peak electric field, the peak magnetic field [10], and the peak Poynting vector [11].

To inhibit breakdowns, recent experiments at SLAC were performed with cooled copper accelerating cavities to cryogenic temperatures. These experiments have shown evidence of 250 MV/m gradients and 500 MV/m peak surface electric fields in X-band copper cavities cooled to 45 K [12]. To un-

derstand the rf properties of the cavities we have constructed experiments to measure the rf surface resistance of cryogenic copper. In this paper we will specifically discuss two measurements of  $Q_0$  in S-band and X-band normal conducting copper structures.

## INTRODUCTION

Early experiments by H. London [13] found that surface resistances in metals for MHz frequencies at cryo temperatures are not accurately predicted by the simple classical model. In the classical model electrons in the conductor are governed by Ohm's Law. The theory to explain this phenomenon, which was called the anomalous skin effect of metals, was laid out by Reuter and Sondheimer [14]. First, we will examine the skin effect in room temperature conductors, and then describe the differences at cryogenic temperatures.

### Normal Skin Effect

First we must assume that Ohm's law holds in the conductor in question, where the current density ( $\vec{J}$ ) is proportional to the electric field ( $\vec{E}$ ) by the conductivity ( $\sigma$ ) of the metal:  $\vec{J} = \sigma \vec{E}$ . Then, in a semi-infinite planar conductor, a perpendicular incident electromagnetic wave in the  $z$  direction with angular frequency  $\omega$  will penetrate the surface and decrease exponentially as the wave travels into the metal, with a characteristic length known as the skin depth ( $\delta$ ) [15];

$$\delta(\omega) = \sqrt{\frac{2}{\mu_0 \sigma \omega}}, \quad (1)$$

where  $\mu_0 = 4\pi \times 10^{-7} \text{H/m}$  is the vacuum permeability. The Maxwell equation  $\epsilon_0 \frac{\partial \vec{E}}{\partial t} = \vec{\nabla} \times \vec{H}$ , ( $\epsilon_0 = 8.85 \times 10^{-12} \text{s}^4 \text{A}^2 / \text{kgm}^3$ ,  $\vec{H}$  is the magnetic field) can be used to find the surface impedance ( $Z_s$ ) and rf surface resistance ( $R_s$ ) since  $\text{Re}(Z_s) = R_s$ , with the assumption displacement currents are negligible. We must make the assumption that the variation of fields in the perpendicular direction is much larger than in variation along the surface of the metal and therefore we can make the assumption,  $\vec{\nabla} = -\vec{n} \frac{\partial}{\partial z}$  [16], where  $\vec{n}$  is the normal to the conductor, which holds in good conductors such as copper. The surface impedance is then:

$$Z_s(\omega) = \sqrt{\frac{\omega \mu_0}{2\sigma}} (1 - i). \quad (2)$$

\* Work Supported by DOE/SU Contract DE-AC02-76-SF00515 and DOE SCGSR Fellowship

<sup>†</sup> acahill@physics.ucla.edu

### Anomalous Skin Effect

Now we will look at the behavior of electrons in low temperature conductors. As the temperature of the metal decreases the mean free path of electrons,  $l = \frac{\sigma \epsilon_0 v_f}{\omega_p^2}$ , increases and the skin depth decreases [17]. In copper  $\omega_p = 1.64 \times 10^{16} \text{ rad/s}$  and  $v_f = 1.58 \times 10^6 \text{ m/s}$ . As the electric field begins to vary on the order of the skin depth, Ohm's Law no longer holds. To find the true electron current the electric field will need to be integrated over the path of the electrons in the metal, which was done in [14] and then reduced to the following in [18]:

$$Z_s(\omega) = -\frac{i\omega l \mu_0}{cF(\omega)}, \tag{3}$$

$$F(\omega) = -\frac{1}{\pi} u \int_0^\infty \ln \left[ 1 + \frac{\xi \chi(t)}{t^2} \right] dt, \tag{4}$$

$$u = 1 + i \frac{\omega l}{v_f}, \tag{5}$$

$$\chi(t) = 2t^{-3}[(1+t^2)\arctan(t) - t], \tag{6}$$

$$\xi = i\alpha u^{-3}, \tag{7}$$

$$\alpha = \frac{3}{2} \left( \frac{l}{\delta(\omega)} \right)^2. \tag{8}$$

The solutions to these equations for copper at different frequencies are shown in Fig. 1.

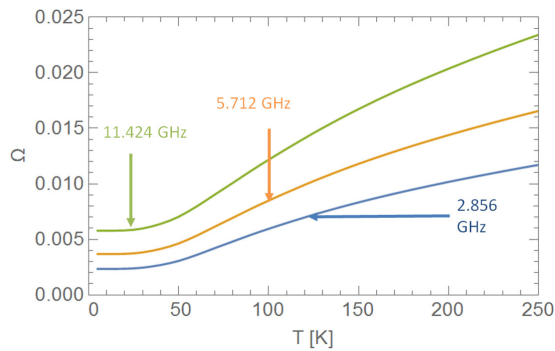


Figure 1: Theoretical comparison of the anomalous skin effect surface resistance in Residual Resistivity Ratio (RRR)=400 Cu at 2.856, 5.712, and 11.424 GHz

### X-BAND MEASUREMENTS

In experiments at SLAC a copper cavity was created that would be placed in a cryostat and used to measure the surface resistivity and  $Q_0$  of materials at temperatures down to 4 K [19]. The original goal was to measure the rf surface resistance of superconducting samples from exotic materials at high power. We took this cavity and used it to measure Cu rf surface resistance at low power. The experiment presented here is a continuation of studies to measure properties of cryogenic copper.

### Cavity Design

The cavity for measuring the rf surface resistance of samples was chosen to operate in the  $TE_{013}$  mode [19]. This mode maximizes the magnetic field on the samples under test, giving them a maximal effect on the  $Q_0$  of the cavity. The cavity was designed to operate near 11.424 GHz.

We define geometric factor,  $G$ , as  $\frac{G}{R_s} = Q_0$ . The geometric factor for a copper cavity shown in Fig. 2 is  $G = 1416$ , attained from simulations using HFSS [20].

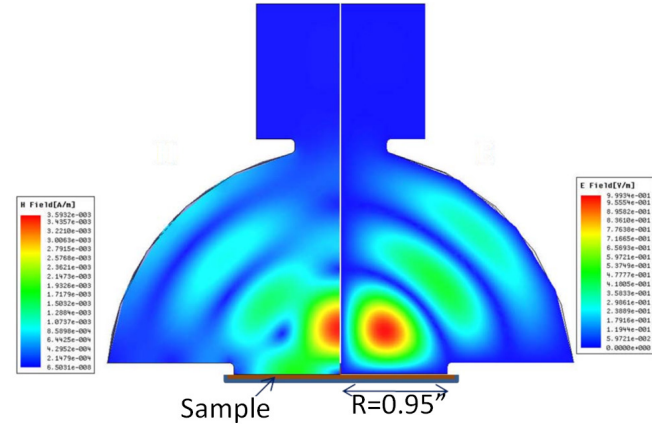


Figure 2: Electric (right half) and magnetic (left half) field maps of the sample testing cavity. Sample plate is located on the bottom [19].

### Methods

We used a network analyzer to measure the reflection of the cavity and an equivalent circuit model to extract the  $Q_0$ . With known geometric factor, we can calculate the rf surface resistance of the copper.

### Results

We ran a temperature scan of the Cu cavity, recording  $Q_0$  every 0.1 K. Results are shown in Fig. 3. The rf surface resistance decreases by a factor of 3.93 from room temperature to 4 K.

### S-BAND MEASUREMENTS

We would like to extend rf breakdown studies to S-band copper cavities. This will also support the TOPGUN project for a cryogenic copper S-band rf photoinjector [21]. Before performing high power tests we would like to measure the rf surface resistance of cryogenic copper.

### Cavity Design

The cavity design chosen for the S-band tests is a pillbox, that will be manufactured from two pieces of copper brazed together (see Fig. 4). The radius of the cavity was chosen so that the  $TM_{010}$  mode will be 2.586 GHz at 20 K. Due to thermal expansion, at room temperature the resonant frequency is 2.847 GHz.

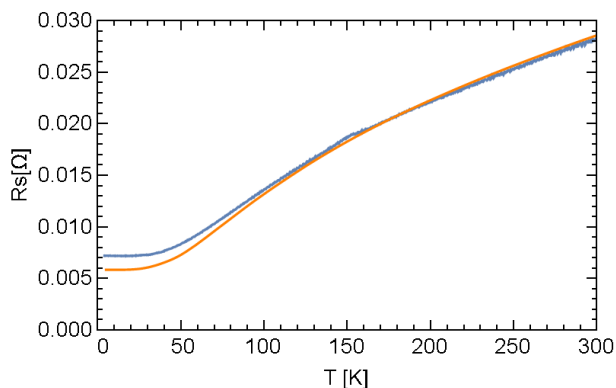


Figure 3: RF Surface resistance of the X-band accelerating cavity (blue), compared to theoretical value (orange) calculated for copper with International Annealed Copper Standard (IACS) 95% and RRR=400.

The length of the cavity was chosen to be 48 mm due to space constraints in the cryostat. To remove degeneracy of the multipole modes we cut a groove in the outside radius that breaks the azimuthal symmetry. To couple rf into the cavity we used two separate antennas, one through the flat wall of the pillbox and the other in the outer diameter. In the first experiment we used only the antenna in the flat wall to couple to the  $TM_{010}$  mode. The other antenna has little effect on the measurement.

The  $Q_0$  of the cavity was calculated to be 18,000 with a geometric factor of 252. The outside coupling of the cavity was tuned by changing the length of the antenna. The calculated surface electric and magnetic fields are shown in Fig. 4.

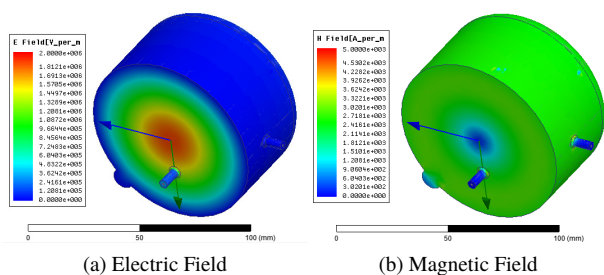


Figure 4: Surface electric and magnetic  $TM_{010}$  fields of the S-band cavity. Fields are normalized to 1 mJ stored energy.

## Results

Two of the S-band cavities were manufactured from different copper stocks and by two separate machine shops, to show the reproducibility of the data. The first cavity was made at SLAC, and the second at UCLA. Data taken from both cavities at 4 K and room temperature is shown in Table 1. We see that the frequency for both cavities was within a few MHz of the design. The measured  $Q_0$  was lower than design by about 5%. The design was done using copper conductivity of  $5.8 \times 10^7$  S/m. Once the coupling antennas

were tuned, the coupling beta reached the designed value of  $\beta = 0.25$  at room temperature. The  $Q_E$  of both cavities varies with temperature. We speculate that this may be caused by the length of the coupling antenna with changing with temperature. The increase in  $Q_0$  from room temperature to 4 K is measured to be 4.82 for the SLAC cavity and 4.78 for the UCLA cavity.

Table 1: Measured Values for the S-band cavities

	SLAC Cav		UCLA Cav	
	4 K	293 K	4K	293 K
$Q_0$	82931	17184	83066	17375
$Q_E$	92249	80118	58272	68014
$f_0$ (GHz)	2.855	2.845	2.856	2.846

**Temperature Scan** We performed temperature scans on both cavities, where the  $Q_0$  was measured every 0.1 K as the cryostat warmed to room temperature from 4 K. The scan on the UCLA cavity stopped after reaching 50 K due to problems with the network analyzer. The cavity from SLAC warmed to 300 K. We calculated the rf surface resistance using the geometric factor,  $G=252$ . In Figure 5, we show the data from these temperature scans compared to the theoretical value.

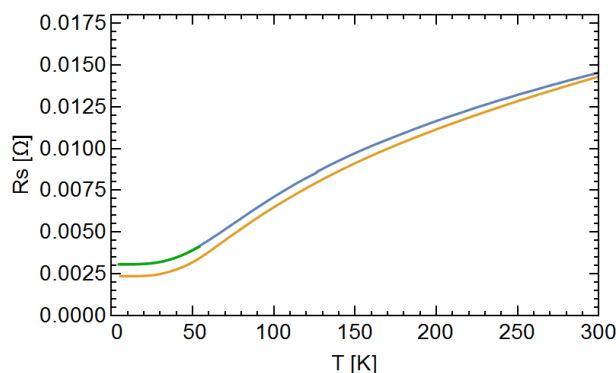


Figure 5: RF Surface resistance of S-band accelerating cavities, SLAC (blue) and UCLA (green) compared to theoretical value (yellow) for copper with IACS 95% and RRR=400.

## DISCUSSION

We measured the rf surface resistance of cryogenic copper at two frequencies. The  $Q_0$  increased by factors of 3.93 for X-band and about 4.8 for S-band from room temperature to 4 K, and thus resistive losses of the cavities fell by the same factors. Theoretical calculated values for RRR=400 and IACS 95% give slightly larger numbers. One possibility to explain the difference is that the RRR of our copper is smaller than we believe, possibly due to the brazing and manufacturing process. This difference could be a topic of future study.

## REFERENCES

- [1] S. Doebert et al., High gradient performance of NLC/GLC X-band accelerating structures in Proceedings of the 21st Particle Accelerator Conference, Knoxville, TN, 2005 (IEEE, Piscataway, NJ, 2005), p. 372
- [2] J. W. Wang, R&D of accelerator structures at SLAC, High Energy Phys. Nucl. Phys. 30, 11 (2006)
- [3] C. Adolphsen, Normal Conducting rf Structure Test Facilities and Results in Proceedings of the 2003 Particle Accelerator Conference, Portland, OR (IEEE, New York, 2003), p. 668.
- [4] V. A. Dolgashev, Progress on high-gradient structures, AIP Conf. Proc. 1507, 76 (2012).
- [5] V. Dolgashev, S. Tantawi, Y. Higashi, and B. Spataro, Geometric dependence of radio-frequency breakdown in normal conducting accelerating structures, Appl. Phys. Lett. 97, 171501 (2010).
- [6] F. Wang, C. Adolphsen, and C. Nantista, Performance limiting effects in X-band accelerators, Phys. Rev. ST Accel. Beams 14, 010401 (2011)
- [7] V. A. Dolgashev and S. G. Tantawi, Simulations of Currents in X-band accelerator structures using 2D and 3D particle-in-cell code in Proceedings of the Particle Accelerator Conference, Chicago, IL, 2001 (IEEE, New York, 2001), p. 3807
- [8] V. Dolgashev and S. Tantawi, Effect of rf parameters on breakdown limits in high-vacuum X-band structures, AIP Conf. Proc. 691, 151 (2003).
- [9] V. A. Dolgashev, High magnetic fields in couplers of X-band accelerating structures in Proceedings of the 2003 Particle Accelerator Conference, Portland, OR (IEEE, New York, 2003), p. 1267.
- [10] V. A. Dolgashev and S. G. Tantawi, RF Breakdown in X-band Waveguides in Proceedings of the 8th European Particle Accelerator Conference, Paris, 2002 (EPS-IGA and CERN, Geneva, 2002), p. 2139.
- [11] A. Grudiev, S. Calatroni, and W. Wuensch, New local field quantity describing the high gradient limit of accelerating structures, Phys. Rev. STAccel. Beams 12, 102001 (2009).
- [12] V. A. Dolgashev, A. Cahill, S. Weathersby, J. Lewandowski, A. Haase, C. Yonedca, S. Tantawi, "Preliminary Results of High Power Tests of Normal Conducting Cryo Cavity" Presented at HG2015 [https://indico.cern.ch/event/358352/contributions/1770594/attachments/1142220/1636464/cryo\\_HG2015\\_V2229\\_14Jun2015.pdf](https://indico.cern.ch/event/358352/contributions/1770594/attachments/1142220/1636464/cryo_HG2015_V2229_14Jun2015.pdf)
- [13] London H. 1940. Proc. R. Soc. A 176 522
- [14] Reuter G E H, Sondheimer E H. 1948. Proc. R. Soc. A 195 336.
- [15] Podobedov B. PRSR AB 12 044401 2009
- [16] J D Jackson. Classical Electrodynamics. 1962
- [17] Matula R A. J Phys. Chem. Red. Data 8 4 1979
- [18] Chambers R G. Proc R. Soc. A 215 481 1952
- [19] J. Guo, S. Tantawi, D. Martin, C. Yoneda. Cryogenic rf Material Testing with a High-Q Copper Cavity. AIP Conference Proceedings 1299, 330 (2010)
- [20] ANSYS HFSS, 3D Full-wave Electromagnetic Field Simulation by Ansoft
- [21] J.B. Rosenzweig, A. Cahill, V. Dolgashev, C. Emma, A. Fukusawa, R. Li, C. Limborg, J. Maxson, P. Musumeci, A. Nause, R. Pakter, R. Pompili, R. Roussel, B. Spataro, and S. Tantawi, Next Generation High Brightness Electron Beams From Ultra-High Field Cryogenic Radiofrequency Photocathode Sources, Preprint, <http://arxiv.org/abs/1603.01657>